Transactions on the Built Environment vol 8, © 1994 WIT Press, www.witpress.com, ISSN 1743-3509

Inelastic responses of pile-soil system to blast loads

H. Hao, T.C. Pan & Z. Zhao
School of Civil and Structural Engineering, Nanyang Technological University, Nanyang Avenue, Singapore 2263

ABSTRACT

This paper presents a numerical method to calculate the elastic and inelastic single pile responses to blast loads. It models the pile-soil system as beam-column elements supported by both horizontal and vertical soil springs of Winkler foundation. The material properties of the beam-column elements are represented by a bi-linear moment-rotation relation. The axial force effect is also considered by including the geometrical stiffness. The pile yielding values are obtained from the axial force and moment interaction curves. A tri-linear force displacement relation is used to model the soil stiffness. The Rayleigh type viscous damping is used to model the energy-loss mechanism of pile and hysteretic damping to model that of soil. The Newmark method with constant average acceleration is used to solve the nonlinear dynamic equation. As a numerical example, the responses of a reinforced concrete pile subjected to a close range TNT explosion is evaluated. The results presented show that the method is efficient and easy to use, and produces reasonable results which can be used in the preliminary design.

INTRODUCTION

The dynamic pile-soil responses to earthquake ground motion excitations have been studied extensively. But many of these studies did not consider the inelastic responses for both pile and soil. Some researchers [1-3] analysed pile responses by studying the pile-soil interaction based on the Winkler assumption. This method considered the inelastic soil behaviour, but did not take into account the inelastic pile responses.

The inelastic behaviour may occur when piles are subjected to

large blast loading at a close range. Rational design procedures should therefore attempt to estimate the amount of inelastic behaviour expected. Based on the report by Bingham, et al [4], not only the soil in a close range of the detonation will yield, but also the piles. Thus, a complete model for the pile-soil system response to blast loads should include the nonlinear inelastic behaviour for both pile and soil. In this paper, a bi-linear moment-rotation relation is used to model the pile nonlinearity, and a tri-linear soil spring is used to model the soil stiffness. The geometric stiffness is also included in the formulation to account for the axial force effect on the pile responses. The axial force-moment interaction curve of pile is used to determine the pile yielding values. For simplicity and without losing accuracy, the mass is lumped at the respective pile nodes in the formulation. The Rayleigh type viscous damping is used to model the energy loss mechanism for pile, whereas the hysteretic type damping for soil. The Newmark method with constant average acceleration assumption is used in the step-by-step integration. The responses of a reinforced concrete pile to the blast loads produced by an underground contained explosion at a close distance are calculated and presented as a numerical example.

PILE MODEL

For a general 2D beam-column element with bending and axial displacement, Figure 1, the force displacement equation in the local coordinate system is

$$\underline{P} = \begin{pmatrix} P_1 \\ P_2 \\ P_3 \end{pmatrix} = \begin{pmatrix} k_{11} & k_{12} & 0 \\ k_{21} & k_{22} & k_{23} \\ 0 & k_{32} & k_{33} \end{pmatrix} \begin{pmatrix} \Delta_1 \\ \Delta_2 \\ \Delta_3 \end{pmatrix} = \underline{k}^P \underline{\Delta} \tag{1}$$

where, for prismatic member with shear deformation $k_{11} = k_{22} = (\frac{4+2\beta}{1+2\beta})\frac{EI}{L}$, $k_{12} = k_{21} = (\frac{2-2\beta}{1+2\beta})\frac{EI}{L}$, and $k_{33} = \frac{EA}{L}$, in which E is the Young's modulus, A is the cross section area, L is the member length, I is the moment of inertia, and $\beta = \frac{6EI}{L^2 A_s G}$, with A_s being the shear area and G the shear modulus.

Equation (1) can be transformed into the global coordinates as shown in Figure 1 by a transform matrix $\underline{B}$,

$$\underline{F} = \underline{B}\underline{k}^p\underline{B}^T\underline{U} \tag{2}$$

where $\underline{F}$ and $\underline{U}$ are nodal force and displacement vectors in the global coordinates.

Accounting for the axial force effects, the geometric stiffness is included in the element stiffness formulation. For each element,

the geometric stiffness in the local coordinate system is

$$\underline{K}^G = \begin{pmatrix} \frac{N}{L} & -\frac{N}{L} & 0 \\ -\frac{N}{L} & \frac{N}{L} & 0 \\ 0 & 0 & 0 \end{pmatrix} \tag{3}$$

where N is the axial force.

A bi-linear moment-rotation relationship is assumed for the pile nonlinear inelastic responses as shown in Figure 1. The yielding value is calculated from the axial force and moment interaction curve.

The viscous damping of the Rayleigh type is used to model the energy-loss mechanism of pile, that is

$$\underline{C}^P = \alpha \underline{M}^P + \beta \underline{K}^P \tag{4}$$

where α and β are constants, and $\underline{M}^P$ and $\underline{K}^P$ are the mass and stiffness matrices of the pile, respectively.

SOIL MODEL

The soil stiffness is represented by springs distributed along the pile length. The stiffness values can either be obtained from the P-Y curve of the soil or approximated by [5]

$$K^i = 2(1+\nu)G_s f \delta^i \qquad i = h, \quad v \tag{5}$$

where ν is the Poisson's ratio, G_s is the shear modulus of the soil, δ^h and δ^v are frequency independent coefficients for the dynamic spring stiffness, in this study $\delta^h = 2.5$ and $\delta^v = 0.6$ are used; and f is a coefficient which depends on the rate of the pressure applied. For a rapid pressure increment resulting from blast loads, f=1.1 should be used [6].

The soil spring stiffness is lumped at the various nodes. For a element with length L connected at node i, its contribution to the lumped spring stiffnesses are

$$k_i^h = K^h L/2 \qquad , k_i^v = K^v L/2 \qquad , k_i^\theta = K^h L^3/30 \tag{6}$$

A tri-linear force displacement relationship is assumed for the soil spring. This assumption allows either a strain hardening or degradating property for the soil stiffness as shown in Figure 2.

The soil distributed damping ratios are

$$C^h = 2d\rho_s V_s[1 + (\frac{V_c}{V_s})^{5/4}]a_0^{-1/4} + 2K^h\frac{\xi}{\omega_1}$$
$$C^v = 2K^v\frac{\xi}{\omega_1} \tag{7}$$

where the first term in C^h accounts for the radiation damping and the second one for hysteretic damping [5]; ξ is the hysteretic damping ratio and ω_1 is the fundamental vibration frequency. The damping coefficient at each node is similarly lumped as the spring stiffness.

DYNAMIC RESPONSE ANALYSIS

The stiffness, mass and damping matrices of all the elements are assembled to form the equilibrium equations of the pile-soil system in matrix form

$$\underline{M}\ddot{\underline{U}} + \underline{C}\dot{\underline{U}} + \underline{K}\underline{U} = \underline{P}(t) \tag{8}$$

where $\underline{M}$ is the lumped mass matrix; $\underline{C} = \underline{C}^p + \underline{C}^s$ is the damping matrix, $\underline{K} = \underline{K}^p - \underline{K}^G + \underline{K}^s$ is the total stiffness matrix, $\underline{P}(t)$ is the external load vector, and $\underline{U}$ is the displacement response vector.

Equation (8) is solved by the step-by-step numerical integration. For this nonlinear dynamic response problem, the Newmark method with constant average acceleration assumption is used because it usually results in stable solutions.

At every integration step, the yielding condition is checked for all nodes of the pile and soil springs. If yielding occurs, the stiffness and the damping matrices are reformulated. As the integration time step is very small, the equilibrium correction approach is used to account for the stiffness changes. The unbalanced forces due to yielding are calculated and then applied to the next time step.

NUMERICAL EXAMPLE

A three layered site with a 20m long, 0.3m by 0.3m, reinforced concrete pile subjected to an assumed quantity of TNT and 100kN axial force at pile head is analysed, Figure 3. The explosive is buried 5m below the surface and 5m from the pile. The explosion is contained and the pressures acting on the pile are calculated based on the technical manual TM-5 [7].

The pile is discretized into 20 elements with 21 nodes, and the bottom of the pile is fixed. The Young's modulus of pile is $E = 32.8GPa$, strain hardening ratio=0.05, shear area=$0.06m^2$,

Poisson ratio=0.33, density=$24kN/m^3$, and damping ratio 0.05. The axial force-moment interaction yielding curve is shown in Figure 4.

The mass is lumped to each of the translational degree of freedom, and no mass for rotational degree of freedom. The initial soil stiffness and damping are obtained from Equations 5 and 7, respectively. The stiffness value of the second portion of the tri-linear model is assumed to be 50% of the corresponding value of the first portion. The stiffness value for the third segment is zero. The yield forces are calculated based on the assumption that $\epsilon_{50} = 0.5\%$ for the first yield force and that $\epsilon = 2\%$ for the second yield force. The hysteretic damping ratio for the soil is assumed to be 8%.

The numerical results show that the fundamental frequency of the pile-soil system is $f_1 = 37.56Hz$, which is controlled by the soil spring stiffness. The pile elements 1, and 15 to 19 yield with the maximum plastic hinge rotation of 0.098rad at node 18 of element 18, this corresponds to the maximum moment of $1.82 \times 10^6 Nm$. The maximum shear force also occurs in element 18 as $2.86 \times 10^6 N$. Elements 15 to 19 yield because they are close to the explosive and subjected to larger impulse forces than other elements. The greatest moment and plastic hinge rotation occur at node 18 where soil properties change abruptly. This change not only affects the soil spring stiffness, but also the impulse forces. Element 20 does not yield because the only rotational restrain at the pile head comes from the soil spring, which leaves the pile head almost free to rotate.

Yielding occurs for the horizontal soil springs at nodes 19, 20 and 21 and the rotational spring at node 21. No vertical soil spring yields because only the static vertical force is appiled. The soil springs corresponding to nodes 19 to 21 yield because of the large horizontal pile displacement.

Figure 5 shows the time histories of some pile response quantities. It can be seen that permanent displacement and rotations occur at the top of pile due to yielding. The rotation at node 19 is larger than those at nodes 20 and 21 initially. This is because node 19 yields under impulse load while nodes 20 and 21 do not. However, rotation of node 21 becomes the greatest in the free vibration phase as the rotations are controlled by rigid body rotation due to different nodal displacement.

The shear force time histories in elements 19 and 20 and moment time histories of nodes 19, 20 and 21 are also shown in Figure 5. The first peaks of the shear force response correspond to the first peak of impulse forces from the direct explosion wave

with 0.01s duration. As the second and third impulse waves due to soil layer reflection are much smaller than the first wave, the response can be considered as free oscillation after 0.01s. Thus the peak shear responses all occur in the free vibration phase. As for the moment response, only node 20 has a peak corresponding to the direct impulse wave. The peak responses for nodes 19 and 21 occur during free vibration phase. This is because the uniform impulse force and uniform soil springs are assumed in each layer. With the initial impulse forces applied, most of the forces are balanced by soil spring and the pile moves rather uniformly. Since node 21 is restricted only by soil rotational spring which is smaller than the pile element flexural rigidity, it is almost free to rotate and therefore a peak moment corresponding to the initial impulse force is expected at node 20.

CONCLUSIONS

A computational method to calculate the pile-soil system responses to blast loads has been presented. It models the pile-soil system as beam-column element on Winkler's foundation. The material properties of pile and soil are represented by a bi-linear and a tri-linear models, respectively. The yield value of pile is obtained from the pile moment-axial force interaction curve. The method can be used to calculate the elastic and inelastic responses of dynamic pile-soil system, as well as the pile node plastic hinge rotations, which can be taken as a measure of pile failure. The method is efficient and can be applied to estimate the pile-soil responses to any transient dynamic load.

REFERENCE

1. Penzien, J., 'Soil-pile-foundation interaction', Earthquake Engineering (Ed. R.L. Wiegel), Prentice-Hall, Englewood Cliffs, 1970.
2. Nogami, T., Otani, J., Konagai, K. and Chen, H-L, 'Nonlinear soil-pile interaction model for dynamic lateral motion', J Eng Mech, ASCE, Vol 118, No. 1, pp89-106, 1992.
3. Matlock, H., Foo, S. H. C., Tsai, C-F. and Lam, I., 'SPASM 8, a dynamic beam-column program for seismic pile analysis with support motion', Fugro. Inc., 3777 Long Beach Boulevard, Long Beach, California 90807, 1979.
4. Bingham, B. L., Walker, R. E. and Blouin S. E., 'Response of pile foundations in saturated soil', Proce Sixth International Sym on Interaction of Nonnuclear Munitions with Structures., pp140-145, 1993.
5. Kavvadas, M. and Gazetas, G. 'Kinematic seismic response and bending of free-head piles in layered soil', Journal of Geotechnique, Vol. 43, No.2, pp207-222, 1993.

6. Hayashi, S., 'Horizontal resistance of steel piles under static and dynamic loads', Proc. 3rd WCEE, 1965.
7. 'TM-5-855-1, Technical manual, fundamentals of protective design for conventional weapons', Headquarters, Department of the US army, 1986.

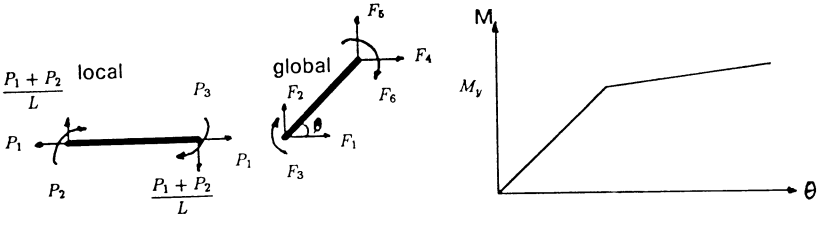

Fig. 1. 2D beam column element and bi-linear model

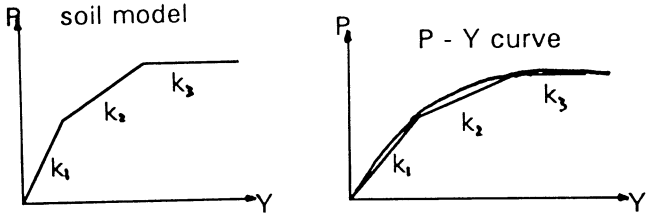

Fig. 2. Tri-linear soil spring model and P-Y curve

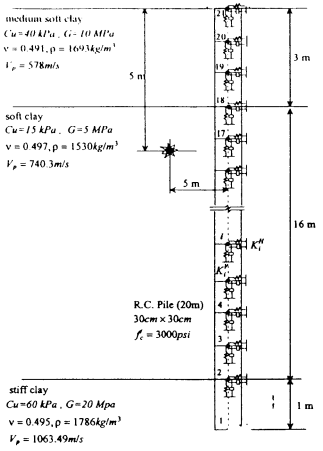

Fig. 3. Pile element and soil profile

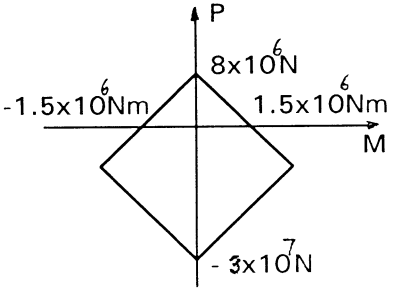

Fig. 4. Moment-axial force interaction curve

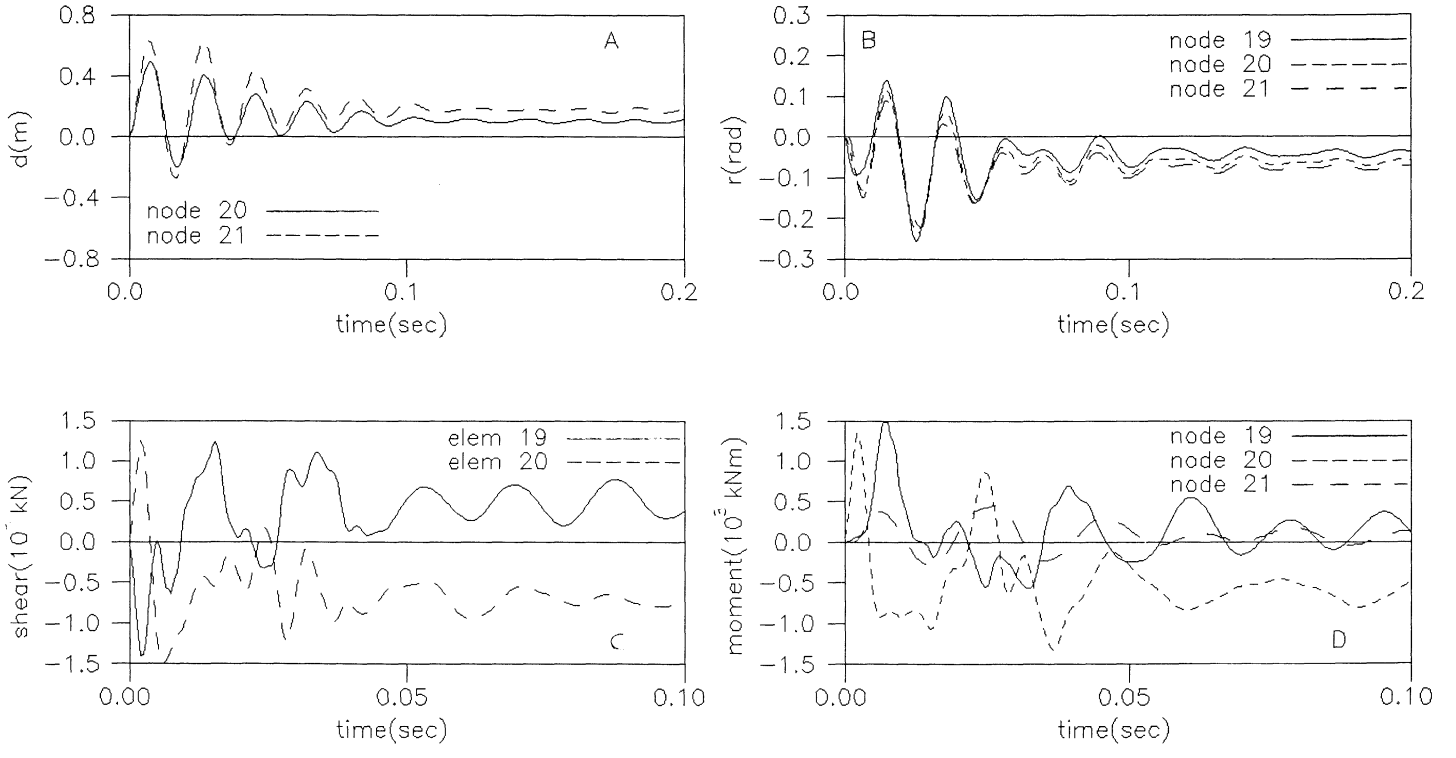

Fig. 5. Pile responses to blast loads, A: horizontal nodal displacement, B: nodal rotations, C: element shear forces, and D: nodal moments